

Effects of Mn Substitution on Magnetic and Electronic Properties of β -SiC Semiconductor

M. Izadifard

Physics department, Shahrood University of Technology

Shahrood, P.O.BoX: 3619995161, Iran

Tel: 98-273-339-5270 E-mail: mizadifard@yahoo.com

M. E. Ghazi (Corresponding author)

Physics department, Shahrood University of Technology

Shahrood, P.O.BoX: 3619995161, Iran

Tel: 98-273-339-5270 E-mail: ebrahim_ghazi@yahoo.com

S. Hosaini

Physics department, Shahrood University of Technology

Shahrood, P.O.BoX: 3619995161, Iran

Tel: 98-273-339-5270 E-mail: smr_hoseini80@yahoo.com

Abstract

Wide band gap semiconductors doped by transition metals are attracting much attention in part because of possible 'spintronics' applications. Using pseudo-potential plane-wave calculations and density functional theory (DFT), we studied effects of doping Mn of various concentrations on the cubic silicon carbide structure (β -SiC). Band structures and density of states (DOSs) were calculated for β -SiC and $\text{Si}_{1-x}\text{Mn}_x\text{C}$ (with $x=0.0313, 0.0625,$ and 0.25). Analyses of the DOSs revealed that the diluted ferromagnetic semiconductor $\text{Si}_{1-x}\text{Mn}_x\text{C}$, i.e. SiC with Mn substituted for Si, should be a half-metal. Our results show spin polarization at Fermi energy (E_f), and a stable ferromagnetic state for $x=0.0625$.

Keywords: Diluted magnetic semiconductors, Spintronics, Semimagnetic semiconductors, Pseudo-potential plane-wave, Spin polarization

1. Introduction

Diluted magnetic semiconductors (DMSs), also referred to as semimagnetic semiconductors, in which magnetic elements are substituted for a few percent of host elements, have been intensively studied due to the potential device applications that utilize both information processing and data storage within one material system (Ohno H. 1998, Wolf S. A. *et al.*, 2001). The devices using DMS compounds work on the basis of spin-based electronics, also known as spintronics. It is widely believed that the ferromagnetism in such materials is carrier-induced, with holes donated by Mn ions mediating a ferromagnetic interaction between the randomly localized Mn spins (Sarma S. Das *et al.*, 2003, Ohno H. *et al.*, 1996). Coupling of carrier spins and localized moments (Mn impurities) gives rise to the unique magnetic and transport properties in DMSs. The origin of this phenomenon is still a subject of intense experimental and theoretical efforts worldwide. Most of the works done to date have widely focused on III-V DMS materials such as (Ga,Mn)As, (In,Mn)As and (Ga,Mn)N with Mn concentrations of about 5 atomic percent, which have demonstrated Curie temperatures limited to 150 K (Ku K. C. *et al.*, 2003). Theoretical calculations predict that semiconductors with small spin-orbit coupling and/or consisting of light elements such as p-type wide band gap materials will have Curie temperatures (T_C) above room temperature, as needed to realize functional devices (Dietl T. *et al.*, 2000). For a successful synthesis of high- T_C ferromagnetic DMSs, it is necessary to understand the origin of ferromagnetism in DMSs. Recently, attempts have been made to fabricate SiC-based DMS compounds by implanting Mn or Fe ions in high doses (Theodoropoulou N. *et al.*, 2001). Some major advantages of SiC over the other wide band gap semiconductors are (i) having available large-sized substrates; (ii) developed single crystal epitaxial growth, (iii) controlled doping possibilities, and (iv)

existence of several polytypes with different band gaps (Harris C. I. *et al.*, 2001, Marsi P. 2002). These advantages make SiC a good candidate for both the spintronics and optoelectronics applications. The main building block of all polytypes of SiC is a tetrahedron consisting of a carbon atom bonded to four silicon atoms, and vice versa (Ching W. Y. *et al.*, 2006, Matos M. *et al.*, 2002).

In this work, we used ultrasoft pseudo-potential plane-wave (USPP) calculations (Vanderbilt D.1990) based on the DFT (Kohn W. *et al.*, 1965) to study the effects of doping Mn of various concentrations on the electronic and magnetic properties of β -SiC, which has a zinc blende structure.

2. Calculation method

In this work, we used the Plane Wave Self Consistent Field, PWscf code, which is in the framework of DFT and is based on the pseudo-potential calculation method. This code is a useful tool for calculating DOSs and band structures of materials. Calculations were first carried out on undoped β -SiC structures including two-atomic unit cell and fcc bravais lattice, and then repeated for Mn-doped samples. The ultrasoft pseudo-potentials with identical approximation for each atom of Si, C, and Mn were chosen, and then in order to start the calculations, the lattice parameters, k-points in the first Brillouin zone, and cut-off energy for electronic wave function were optimized. Self and non-self consistent calculations were carried out using these optimized values. Total energies for the 3.13%, 6.25%, and 25% Mn concentrations were calculated.

3. Results and discussion

Starting with the undoped sample, a unit cell with two-atomic basis and fcc Bravais lattice was chosen. The optimized values for cut-off energy and lattice parameter were 28 Ry and 8.28 a.u., respectively. The optimized lattice parameter is in agreement with the reported experimental value, which is 8.23 a.u. (Madelung O. *et al.*, 1982, Gubanov V. A. *et al.*, 2001). Figure 1 shows the calculated band structure for β -SiC along the high symmetry direction in the first Brillouin zone, which is in accordance with the other results (Ohno H. 1998, Ching W. Y. *et al.*, 2006, Matos M.2002). As it could be seen in the figure, this semiconductor has an indirect band gap. Maximum of the valence band is at k-point of Γ ($k=0, 0, 0$), and minimum of the conduction band is at X ($k=2\pi/a, 0, 0$). The value for this indirect band gap, E_g , is 1.37 eV, and the Fermi energy, E_f , the highest occupied level, is 9.27 eV. The value obtained for the band gap is in the range of reported values (Ching W. Y. *et al.*, 2006).

The calculated parameters of interest are tabulated in Table 1. The calculated total density of states (TDOSs) and partial density of states (PDOSs) for 3s and 3p orbitals of Si and for 2s and 2p orbitals of C are shown in Figures 2, 3(a), and 3(b). As shown in Figure 2, valence band region for β -SiC is separated by a small gap. The lower part comes from bonding between C:2s and Si:3s states, whereas the upper part comes from bonding of Si:3p and C:2p states.

In Figures 2 and 3, the zero energy level was chosen at maximum of the valence band. Since the C:2p and Si:3p states are mostly distributed around the valence band edge, the p orbitals are likely to occupy states near the Fermi energy. The states which are distributed at the edge of the conduction band are mixture of all the Si:3p,3s and C:2p,2s states. Figure 3(b) shows that DOSs related to Si atoms are higher than those for C atoms.

Manganese doping causes replacement of atoms from their equilibrium positions and change of lattice parameters due to interactions between atoms. Thus we had to minimize the interactions and interatomic forces by use of relaxation calculations. The self-consistent calculations were carried out to achieve the interatomic forces of the order of 0.0136 eV/a.u (minimum value 0.001 Ry/a.u). To study the effects of Mn doping, we considered three atoms (Si, C, and Mn) in our calculations. We had to substitute one of the Si or C atoms for Mn. We chose to replace Si with Mn because of its higher ferromagnetic state stability (Kim Y. S. *et al.*, 2004). By selecting 8 unit cells with cubic Bravais lattice including one Mn atom, concentration of Mn reached 25%. After the optimization process, cut-off energy of 28 Ry and lattice parameter of 8.28 a.u. were obtained. In a similar way, we chose a 2x2x2 supercell with 64 atoms. By replacing one Si atom for a Mn atom, concentration of Mn reached 3.13%. By replacing two Si atoms for two Mn atoms, concentration of Mn reached 6.25%. The calculated TDOSs for the spin-up and spin-down states with different Mn concentrations are shown in Figures 4(a), 4(b), and 4(c). Zero energy level in these figures coincides the Fermi energy.

As shown in these figures, TDOSs near Fermi energy have only the spin-up state, which means that the electron spins are completely polarized. Thus spin-up states have metallic behavior and spin-down states have semiconductor behavior. According to the figures, maximum spin-up states at Fermi energy occurs for the Mn concentration of 6.25%. The 3d local DOSs for Mn atoms of different concentrations are shown in Figures 5 and 6. Since d electrons of Mn atoms occupy states near the Fermi level, the electronic structure of β -SiC:Mn

depends on the characteristics of the partially filled d-orbitals. These d states can be coupled with sp^3 dangling bonds of Si, resulting in a half-metallic band structure in which the Fermi level lies in the energy gap of the minority states and thus the electrons are fully spin-polarized at E_f (Kim Y. S. *et al.*, 2006). Calculated magnetic moments for the three Mn concentrations are listed in Table 2; these values are in good agreement with the reported values (Madelung O. *et al.*, 1982). A high magnetic moment shows a stable ferromagnetic phase in SiC:Mn.

4. Conclusion

In this work, we used the pseudo-potential plane-wave method and the DFT to study effects of doping Mn of various concentrations on the β -SiC structure. Band structures and DOSs were calculated for pure β -SiC and $Si_{1-x}Mn_xC$ (with $x = 0.0313, 0.0625, \text{ and } 0.25$). The calculated band structure for β -SiC showed that this semiconductor has an indirect band gap of E_i , equal to 1.37 eV.

Analyses of total DOSs of $Si_{1-x}Mn_xC$ near Fermi energy revealed that only the spin-up state exists, which means that the electron spins are completely polarized. Thus spin-up states have metallic behavior and spin-down states have semiconductor behavior. According to the results, maximum spin-up states at Fermi energy occurs for the Mn concentration of 6.25%. The calculation of 3d local DOSs for Mn atoms of different concentrations indicated d electrons of Mn atoms occupy states near the Fermi level. Our calculations showed a spin polarization at E_f and a stable ferromagnetic state for the Mn concentration of 6.25%.

References

- Ching W. Y., Nianxu Y., Rulis P., & Ouyang L. (2006). The electronic structure and spectroscopic properties of 3C, 2H, 4H, 6H, 15R and 21R polymorphs of SiC. *Materials Science and Engineering*, A 422, 147-156.
- Dietl T., Ohno H., Matsukura F., Cibert J., & Ferrand D. (2000). Zener Model Description of Ferromagnetism in Zinc-Blende Magnetic Semiconductors. *Science*, 287, 1019.
- Gubanov V. A., Boekema C., Fong C. Y. (2001). Electronic structure of cubic silicon-carbide doped by 3d magnetic ions. *Applied Physics Letter*, 178, 2.
- Harris C. I., Savage S., Konstantinov A., & Bakowski M. (2001). Progress towards SiC products. *Applied Surface Science*, 184, 393.
- Kim Y. S., Kim H. & Chung Y. C. (2004). Magnetic and half-metallic properties of Cr doped β -SiC. *Key Engineering Materials*, 264-268, 1237-1240.
- Kim Y. S., Chung Y. C., & Yi S. C. (2006). Electronic structure and half-metallic property of Mn-doped β -SiC diluted magnetic semiconductor. *Materials Science and Engineering*, B 126, 194-196.
- Kohn W. & Sham L. J. (1965). Self-Consistent Equations Including Exchange and Correlation Effects. *Physics Review*, 140, A1133-A1138.
- Ku K. C., Potashnik S. J., Wang R. F., Chun S.H., Schiffer P., Samarth N., Seong M.J., Mascarenhas A., Johnston-Halperin E., Myers R. C., Gossard A. C., & Awschalom D. D. (2003). Highly enhanced Curie temperature in low-temperature annealed [Ga,Mn]As epilayers. *Applied Physics Letter*, 82, 2302.
- Madelung O., Schulz M., & Weiss H. (1982). *Landolt-Bornstein New series group III*, vol.17a, springer verleg, New York.
- Marsi P. (2002). Silicon carbide and silicon carbide-based structures: The physics of epitaxy. *Surface Science Report*, 48, 1.
- Matos M. (2002). Electronic structure of several polytypes of SiC: a study of band dispersion from a semi-empirical approach. *Physica*, B 324, 15-33.
- Ohno H., Shen A., Matsukura F., Oiwa A., Endo A., Katsumoto S., & Iye Y. (1996). (Ga,Mn)As: A new diluted magnetic semiconductor based on GaAs. *Applied Physics Letter*, 69, 363.
- Ohno H. (1998). Making Nonmagnetic Semiconductors Ferromagnetic. *Science*, 281, 951.
- Sarma S. Das, Hwang E. H., & Kaminski A. (2003). Temperature-dependent magnetization in diluted magnetic semiconductors. *Physics Review*, B 67, 155201.
- Theodoropoulou N., Hebard A. F., Chu S.N.G., Overberg M. E., Abernathy C.R., Pearton S. J., Wilson R.G. & Zavada J. M. (2001). Magnetic Properties of Fe- and Mn-Implanted SiC. *Electrochemical and Solid State Letters*, 4, G119.

Vanderbilt D. (1990). Soft self-consistent pseudopotentials in a generalized eigenvalue formalism. *Physics Review*, B 41, 7892.

Wolf S. A., Awschalom D., Buhrman R. A., Daughton J. M., molnar S.Von, Roukes M. L., Chtchelkanova A.Y., & Treger D. M. (2001). Spintronics: A Spin-Based Electronics Vision for the Future. *Science*, 294, 1488.

Table 1. Calculated parameters of interest for β -SiC

β -SiC	Our results	Other results
Direct band gap (eV)	5.56	4.86 [10]
Indirect band gap (eV)	1.37	1.317 [16], 1.602 [10]
Width of upper valence band (eV)	8.93	8.59 [10]
Width of lower valence band (eV)	5.65	5.38 [10]
Width of conduction band (eV)	18.25	-

Table 2. Calculated total magnetic moments and spin band gaps for β -SiC

Mn doping (%)	E_f (eV)	Total magnetization (μ_B /cell)	$E_f - E_{VBM}$ (eV)	$E_{CBM} - E_f$ (eV)	Spin down band gap(eV)
3.13%	10.84	3.05	1.2	0.34	1.54
6.25%	10.94	3.00	1.12	0.26	1.38
25%	10.76	3.00	1.96	0.27	2.23

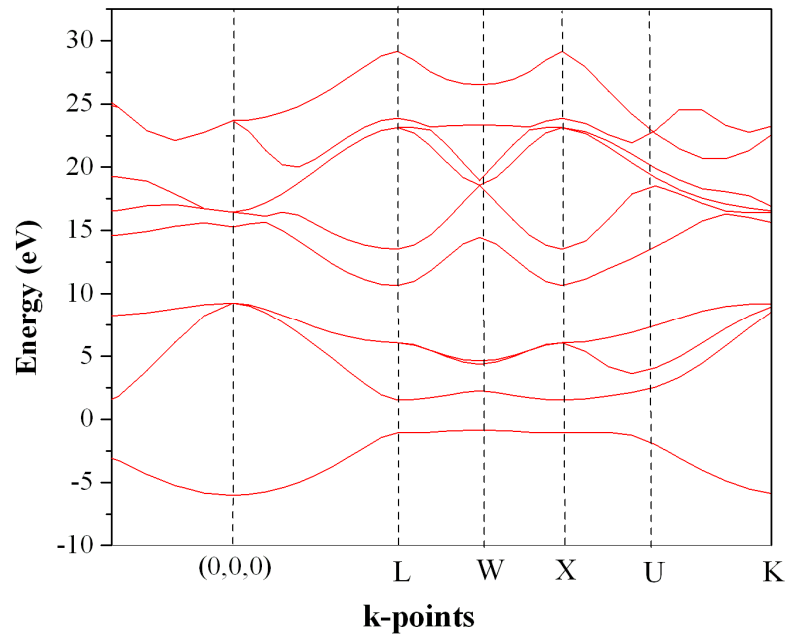


Figure 1. Calculated electronic band structure for β -SiC

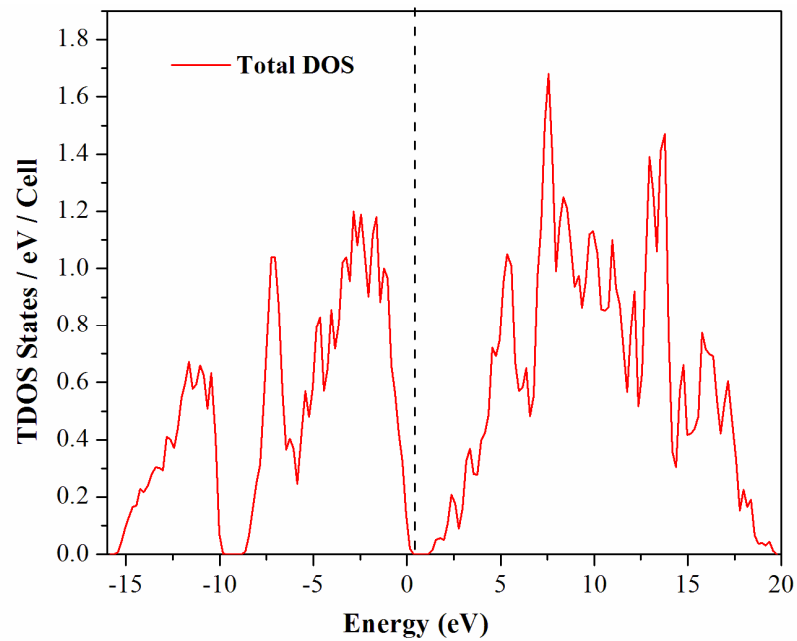


Figure 2. Calculated TDOS for β -SiC structure. The zero energy level corresponds to maximum of the valence band

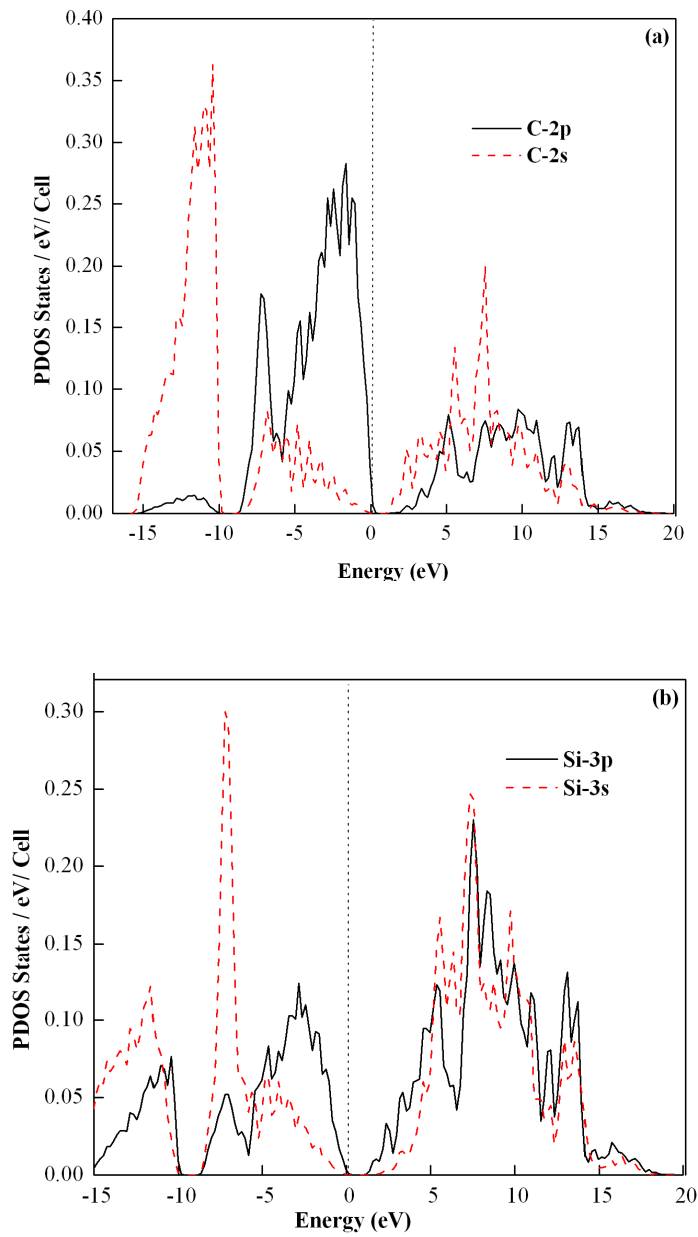


Figure 3. Calculated PDOSs for (a) C:2s and C:2p; and (b) Si:2s and Si:2p

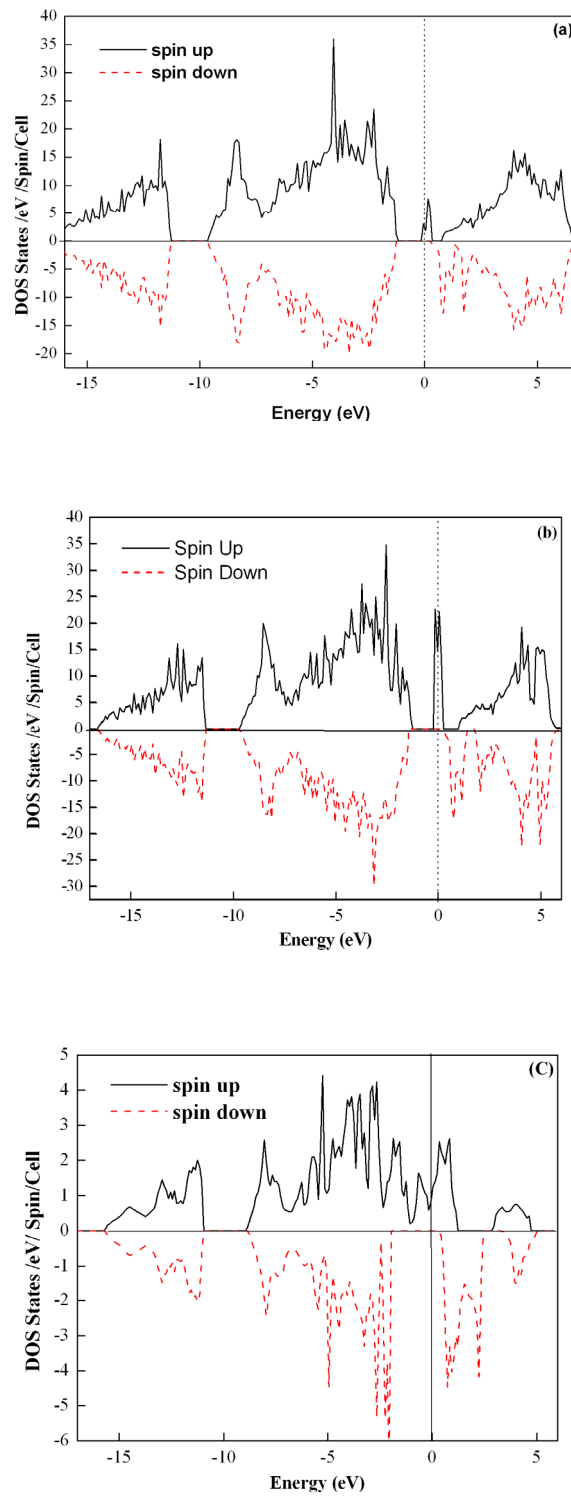


Figure 4. Calculated TDOSs for (a) 3.13% Mn, (b) 6.25% Mn, and (c) 25% Mn.

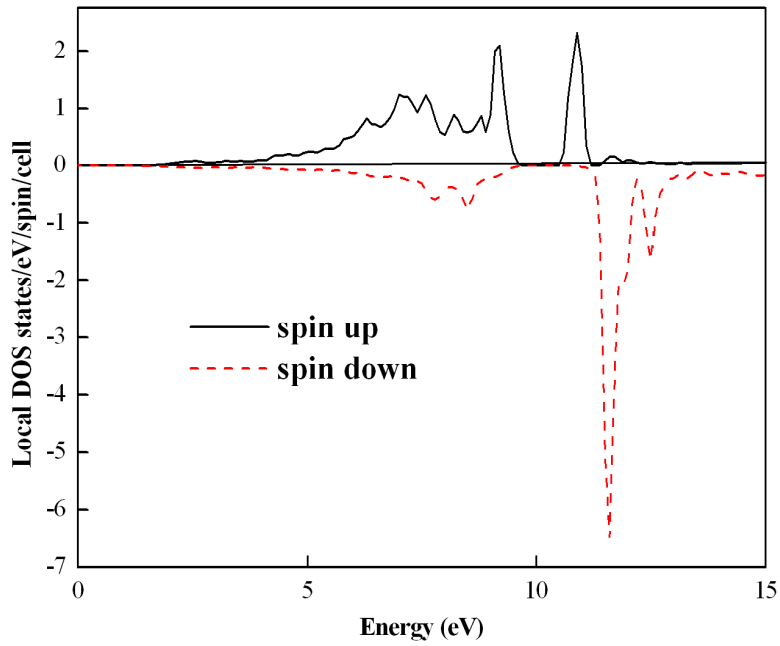


Figure 5. 3d local DOSs for Mn concentration of 3.13%

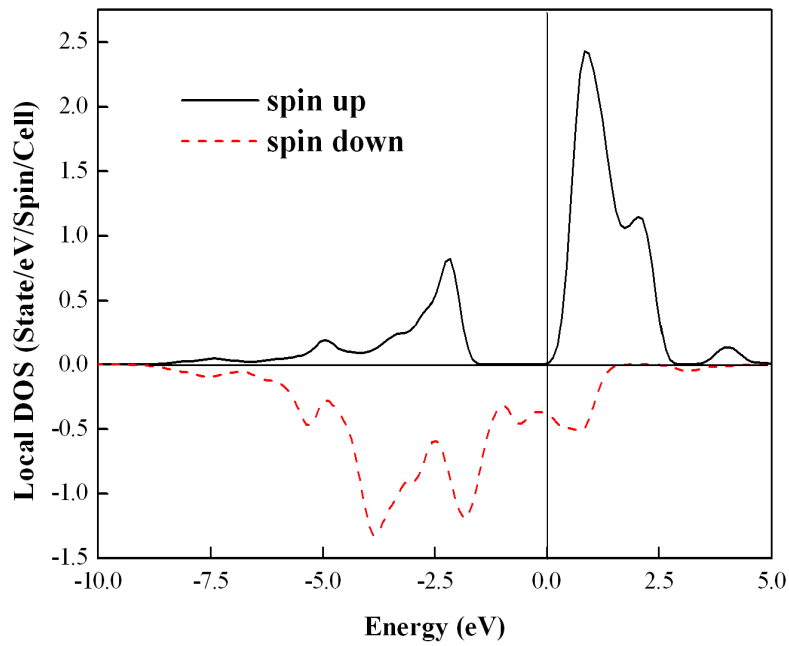


Figure 6. 3d local DOSs for Mn concentration of 25%